Journal of Materials Research and Technology 30 (2024) 1641–1649

Contents lists available at ScienceDirect

Journal of Materials Research and Technology

journal homepage: www.elsevier.com/locate/jmrt

Evolution mechanism of microstructure and microhardness of Ti–6Al–4V alloy during ultrasonic elliptical vibration assisted ultra-precise cutting

Rongkai Tan [a,b,*], Shijing Jin [a], Shuangquan Wei [a], Jiacheng Wang [a], Xuesen Zhao [c], Zhanfeng Wang [d], Qi Liu [e], Tao Sun [c]

[a] Key Laboratory of Conveyance and Equipment of Ministry of Education, East China Jiaotong University, Nanchang, 330013, PR China
[b] Jiangxi Province Engineering Research Center of Drug and Medical Device Qualit, NMPA Key Laboratory of Quality Evaluation of Traditional Chinese Patent Medicine, Jiangxi Institute for Drug Control, Nanchang, 330029, PR China
[c] Center for Precision Engineering, Harbin Institute of Technology, Harbin, 150001, PR China
[d] School of Mechanical and Electrical Engineering, Suqian University, Suqian, 223800, PR China
[e] Department of Design, Manufacturing and Engineering Management, University of Strathclyde, Glasgow, G1 1XQ, UK

ARTICLE INFO

Keywords:
Microstructure
Microhardness
Ti–6Al–4V alloy
Ultra-precision cutting
Ultrasonic elliptical vibration assisted cutting

ABSTRACT

The ultra-precision Ti–6Al–4V alloy parts are growing used in medical and aerospace industries, and which always work in the extreme working conditions such as high temperature, high pressure, and variable load. Thus, the requirements for machining accuracy and surface quality of parts are getting higher and higher. The ultrasonic elliptical vibration assisted cutting (UEVC) technology has been proved to be an effective method for the ultra-precision machining of Ti–6Al–4V alloy. However, in the UEVC process, the evolution mechanism of microstructure and microhardness, which directly affect the service performance and life, is unrevealed. In this paper, the comprehensive investigations of microstructural plastic deformation, grain refinement, phase transformation and microhardness of machined surface layer under conventional cutting (CC) and UEVC processes are carried out. The experimental results indicated that, due to the effects of UEVC technology, the plastic deformation area show obvious compression deformation, the depth of plastic deformation is less than 10 μm, there is no obvious phase transformation on the machined surface layer material, and the hardening rate of machined surface is more than 20%. These findings show the UEVC technology has a unique influence on the microstructure and microhardness of Ti–6Al–4V alloy, which have important implications for the cutting parameter design of ultra-precision Ti–6Al–4V alloy parts.

1. Introduction

Ti–6Al–4V alloy is a typical titanium alloy with a duplex microstructure (α & β), which is one of the most commonly used titanium alloy in medical and aerospace industries, because of its excellent properties such as: high toughness, high strength to weight ratio, high yield stress, corrosion resistivity and good biocompatibility [1–4]. With the rapid development of science and technology, the requirements for machining accuracy and surface quality of titanium alloy parts are getting higher and higher, and the demand for ultra-precision machining of titanium alloy is becoming urgent [5–7]. Moreover, the higher requirements about the corrosion resistance, wear resistance, and fatigue resistance of titanium alloy parts are put forward under extreme working conditions such as high temperature, high pressure, and variable load [8,9]. However, Ti–6Al–4V alloy has been considered to be a typical difficult-to-machine material owing to its inherent properties such as high chemical activity, low elastic modulus and low thermal conductivity [10–12]. The ultrasonic elliptical vibration cutting (UEVC) technology has been proved to be an effective method for the ultra-precision cutting of difficult-to-machine materials such as steel, Inconel 718 and tungsten alloy [13–15]. Moreover, in our previous work, the ultra-precision finished surface of Ti–6Al–4V alloy has been obtained, thanks to the application of UEVC technology [7,16–18]. Significantly, in the ultrasonic elliptical vibration assisted ultra-precise cutting process, the large strain and high strain rate would occur in the machined surface layer because the cutting tool has high frequency and large stress impact on the machined surface, which result in obvious change of microstructure and microhardness [19]. The microstructure and

* Corresponding author. Key Laboratory of Conveyance and Equipment of Ministry of Education, East China Jiaotong University, Nanchang, 330013, PR China.
E-mail addresses: tanrongkai17@163.com (R. Tan), taosun@hit.edu.cn (T. Sun).

https://doi.org/10.1016/j.jmrt.2024.03.214
Received 29 January 2024; Received in revised form 1 March 2024; Accepted 27 March 2024
Available online 28 March 2024

microhardness of the machined surface have a great influence on the fatigue resistance, corrosion resistance, crack resistance and wear resistance of the titanium alloy part, which directly affect the service performance and life [20–22]. Thus, it is necessary to carry out the research on the evolution mechanism of microstructure and microhardness of Ti–6Al–4V alloy during ultrasonic elliptical vibration assisted ultra-precise cutting for achieving the high performance and high precision production of Ti–6Al–4V alloy part.

Tremendous research have been conducted to investigate the microstructure evolution, grain evolution and microhardness change of the Ti–6Al–4V in machined surface [23–27]. Safari et al. studied the changes of microstructure and microhardness with the machined surface of titanium alloy under different machining parameters. And their research results pointed out that the higher cutting speed and feed rate enhanced the subsurface alteration and resulted in considerable plastic deformation and increscent microhardness value [25]. PatilSafari et al. researched the plastic deformation and microhardness in subsurface after dry cutting Ti–6Al–4V alloy. They observed that when the cutting parameters are small, the work hardening effect is obvious and the plastic deformation is obvious. But, when the cutting parameters are large, the thermal softening is stronger than the work hardening, which becomes the main factor affecting the microhardness of machined surface [26]. Rotella et al. [27] researched the microscopic characteristics of titanium alloy machined surface under three machining conditions: low temperature, micro-lubrication and no cooling. The experimental results show that the grain refinement of the machined surface is very obvious under the three machining conditions, and it is significant with the increase of cutting speed and feed rate. They considered that high strain energy and high temperature can obviously promote the recrystallization of the material and inhibit the growth of grain. Wang et al. [28] used the finite element method to study the changes of grain size and microhardness of Ti–6Al–4V alloy during high-speed cutting. The results show that the cutting speed is a significant factor affecting the grain size and microhardness, and the high temperature can significantly promote the dynamic crystallization. Moussaoui et al. [29] analysed the effect of milling on the metallurgical parameters of Ti–6Al–4V alloy. They pointed out that there is slight softening of the machined surface layer during milling, dynamic recrystallization is the main factor leading to grain refinement, and large grain structure led to the reduction of microhardness. Bai et al. [30] studied the grain size of Ti–6Al–4V alloy under one-dimensional ultrasonic vibration-assisted cutting and traditional cutting methods. And the results pointed out that, compared with the traditional cutting surface, the average grain size of the one-dimensional ultrasonic vibration assisted cutting surface is larger and the variation is smaller. Moreover, the addition of ultrasonic vibration assisted technology significantly changes plastic deformation and microhardness in subsurface of Ti–6Al–4V alloy [31–33].

In addition, it is worth noting that Ti–6Al–4V alloy is prone to material phase transition in the plastic deformation region under the coupling intense of cutting heat and cutting force. Zhang et al. [34] analysed the relationship between material phase transformation and machining parameters in the cutting process of Ti–6Al–4V alloy, and pointed out that high temperature in the cutting process is the main factor leading to material phase transformation. Pan et al. [35] studied the effect of machining parameters on the surface microstructure of Ti–6Al–4V alloy during high-speed machining, and the experimental results showed that the volume fraction of β phase increased with the increase of machining speed and feed rate. The research results of Wang and Liu [36] show that the transition from α to β phase is easy to occur in the transient pressure heating process, and the transition from β to α phase will occur in the rapid cooling stage. In addition, the research results of Wang et al. [37] also show that material phase transition exists during the cutting process of Ti–6Al–4V alloy, and the volume fraction of β phase increases with the increase of cutting speed and cutting depth. These results imply that during the processing of Ti–6Al–4V alloy, there are changes in the grain morphology, grain size, material metallography and microhardness of the machining surface, and these characteristics have a decisive impact on the performance of parts. However, the research on the evolution mechanism of microstructure and microhardness of Ti–6Al–4V alloy is mainly concentrated in the field of CC process, and there are few reports about the ultra-precision cutting of Ti–6Al–4V alloy. Moreover, it has been shown that ultrasonic vibration has a unique influence mechanism on the grain size of Ti–6Al–4V alloy. Prior to this study, the evolution mechanism of microstructure of Ti–6Al–4V alloy during ultra-precise cutting with UEVC technology has not been reported.

The purpose of this work is to reveal the evolution mechanism of microstructure and microhardness of Ti–6Al–4V alloy during ultrasonic elliptical vibration assisted ultra-precise cutting, and also aimed to promote the high performance and high precision production of Ti–6Al–4V alloy part. The outline of the paper is organized as follows. The principle of UEVC technology is expound, and the experimental setup and procedures are introduced in Section 2. Then, the comprehensive investigations of microstructural plastic deformation, grain refinement, phase transformation and microhardness of machined surface layer under CC and UEVC processes are carried out in Section 3. The conclusions are given in Section 4.

2. Materials and methods

2.1. The UEVC principle

The schematic illustration of UEVC process is displayed in Fig. 1. In the UEVC process, the cutting tool path is a spiral curve in the *xoz* plane formed by the nominal cutting direction (i.e., *x*-axis) and the cutting depth direction (i.e., *z*-axis). The vibration amplitudes in the *x* and *z* directions are *a* and *b*, respectively. The vibration frequency is *f*, the phase shift is θ, and the nominal cutting speed is V_c. Thus, the tool locus can be described as following:

$$\begin{cases} x(t) = a\cos(2\pi ft) - V_c t \\ z(t) = b\cos(2\pi ft + \theta) \end{cases}. \tag{1}$$

Significantly, the ratio of the nominal cutting speed to the peak horizontal vibration speed is an important parameter in the UEVC process. In this study, this ratio is named as R_S. And R_S can be written as:

$$R_S = \frac{V_c}{2\pi fa}. \tag{2}$$

In the ultra-precision cutting process, the R_S is usually set to be less than one-twelfth [38]. Therefore, the cutting process is intermittent, and the tool only contacts with the workpiece during a short time period (t_0-t_4). During the time period (t_0-t_1), the cutting edge has the large stress

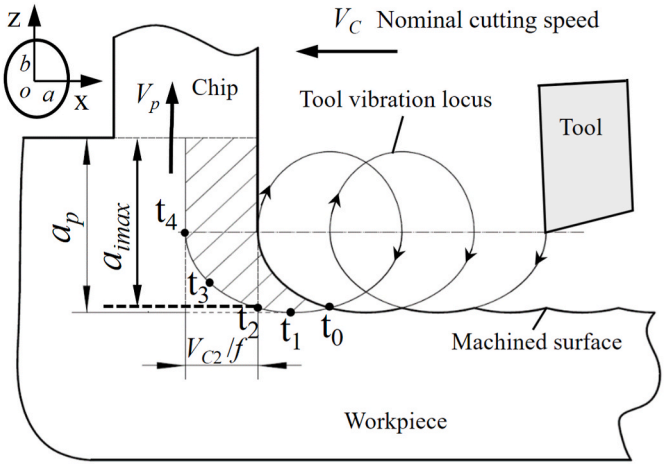

Fig. 1. Schematic of the UEVC process.

impact effect on the machined surface, thereby resulting in the obvious change of microstructure and microhardness. During the time period (t_1-t_2), the extrusion effect of the cutting edge on the machined surface is gradually weakened [39]. The UEVC technology has a unique influence on the microstructure and microhardness of the Ti–6Al–4V alloy machined surface. Hence, it is necessary to further study the evolution mechanism of microstructure of Ti–6Al–4V alloy during ultra-precise cutting with UEVC technology for enhancing the corrosion resistance, wear resistance, and fatigue resistance of ultra-precise Ti–6Al–4V alloy part.

2.2. Experimental setup for cutting process

The experimental setup shows in Fig. 2. The T-type home-made ultra-precision machine tool is used, which has an aerostatic spindle and two horizontal hydrostatic sideways. The workpiece is affixed to the aerostatic spindle by vacuum sucker, the aerostatic spindle is assembled on the x-axis sideway. The UEVC device is fixed on the high-precision adjustment platform, which is used to achieve the height adjustment of the UEVC device and positioned on the z-axis. Fig. 2(b) shows the schematic of the UEVC device, which is work with the 3rd resonant mode of longitudinal vibration and the 6th resonant mode of bending vibration. Thus, the elliptical trajectory is generated at the tool tip. It should be noted that the UEVC device is a traditional tool holder when it is not powered, and more details on the UEVC device can be found in our previous work [40].

The samples are Ti–6Al–4V alloy round pie with the diameter of 50 mm and the height of 20 mm, and the cutting area is set as a 2 mm ring. The pre-turning is first completed without elliptical vibration. After that, a series of experiments are carried out, and the experimental parameters are shown in Table 1. The experimental parameters were selected based on our previous works [7,16–18]. Remarkably, our previous study has shown that during ultrasonic elliptical vibration-assisted ultra-precision cutting of titanium alloy, the tool wear is low and ultra-precision finished surface of titanium alloy with 1260 mm^2 can be realized [18]. Thus, the tool wear is not considered in this study, because of the cutting area is small (about 301.6 mm^2).

2.3. Experimental setup for microstructural characterization test

Fig. 3 shows the sample preparation for observation and assessment of the microstructure specimens of the machined surface layer. After polishing and etching, the microstructure of machined surface layer are observed with the metallographic microscope (VHX-1000E). The thickness of plastic deformation layer (PD layer) is determined by the grain deformation information of machined surface layer. Furthermore, the grain refinement and phase transformation of machined surface layer are further analysed by the information of metallographic structure.

Table 1
Experimental parameters.

Cutting method		CC process	UEVC process
Vibration parameters	Vibration frequency (kHz)	–	29.75
	Amplitude in cutting direction (μm)	–	6
	Amplitude in cutting depth direction (μm)	–	4
	Phase shift difference (°)	–	150
Cutting parameters	Rotational speed (r/min)	480	4/8/16
	Feed rate (μm/r)	5	5
	Depth of cut (μm)	5	5
Cutting tool	Material	Polycrystalline diamond	
	Rake angle (°)	0	
	Clearance angle (°)	11	
	Radius (mm)	0.8	
Workpiece	Material	Ti–6Al–4V alloy	
	Dimension (mm)	$\Phi 50 \times L20$	
	Microhardness (HV)	323	
Coolant		Air cooling	

The β phase grain and α phase grain of Ti–6Al–4V alloy usually show different colour under the microscope, with the β phase grain being darker and the α phase grain being brighter, as shown in Fig. 4. The proportion of α phase grain and β phase grain can be obtained by digitizing the colour in the metallographic diagram. In order to further study the relationship between different depth and grain size of the machined surface layer, the average grain size is calculated by using the scribing method, and the accuracy of this method has been confirmed by Bai et al. [30]. It is worth noting that the morphology of the β phase grain is not conducive to the measurement of grain size, so only the α phase grain size with equiaxed or coarse strip structure is counted in this paper. The test lines are set away from the machined surface 5 μm, 15 μm, 25 μm, 35 μm and 45 μm respectively.

The microhardness of machined surface layer are tested with the microhardness tester (HXD-1000TM). The test load is set as 0.245 N, and the loading force is maintained for 10s. The microhardness value of the tested material can be automatically calculated by microhardness meter based on the length value of the diagonal indentation. Fig. 5 shows the microhardness testing schematic diagram. The microhardness testing starts from the position that away from the machined surface is 10 μm. The spacing between the two groups of test points is 10 μm in the depth direction and 15 μm in the transverse direction. Moreover, as shown in Fig. 5, the two groups of test points are misaligned in a Z-shape. The microhardness test is carried out successively along the cutting depth direction until the obtained microhardness value does not change. Three microhardness tests are performed at the same depth, the transverse spacing is 30 μm, and the averaging value is recorded. Moreover, the hardening rate of titanium alloy machined surface has been studied. The hardening rate refers to the degree of hardening of the machined

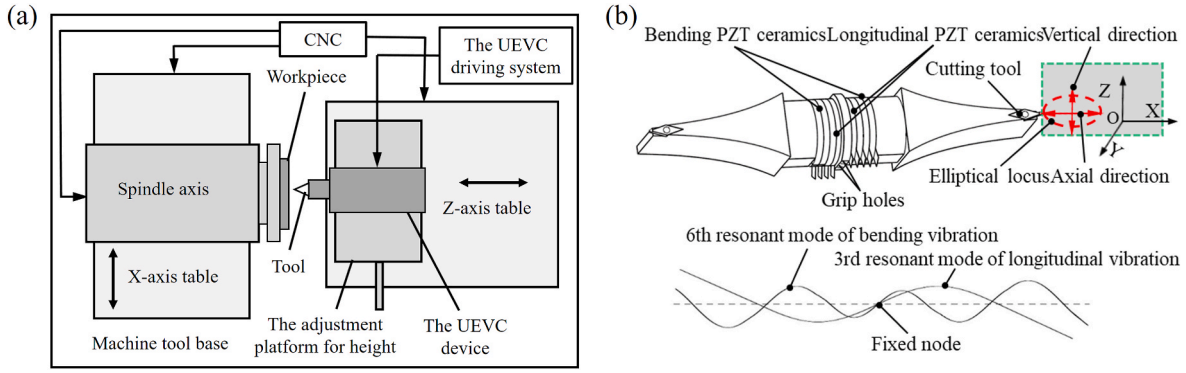

Fig. 2. (a) Schematic of the experimental platform. (b) Schematic of the UEVC device and its working modes.

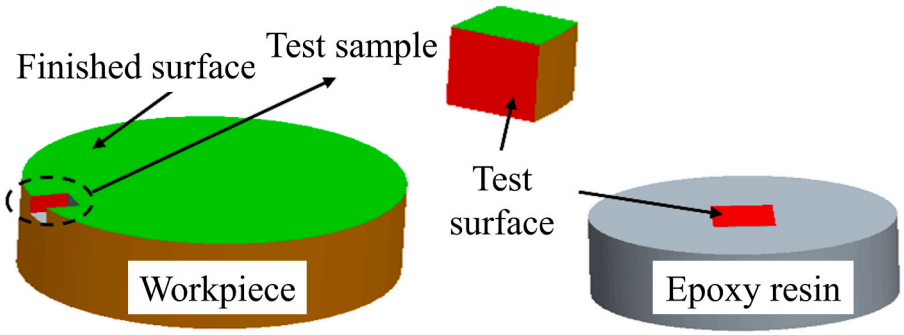

Fig. 3. Schematic of the sampling of test samples.

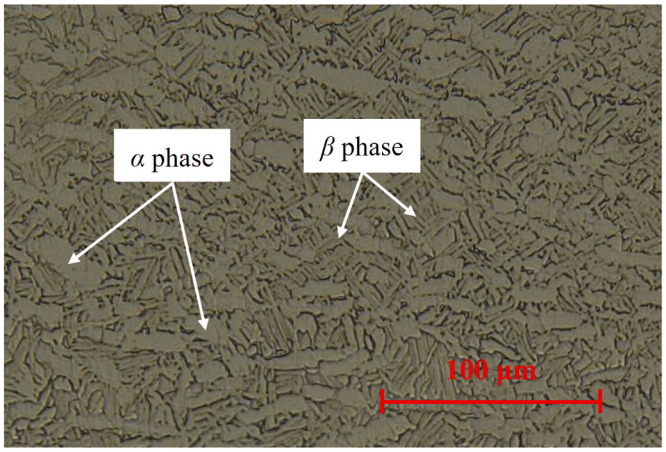

Fig. 4. Microstructure of Ti–6Al–4V alloy used in this study.

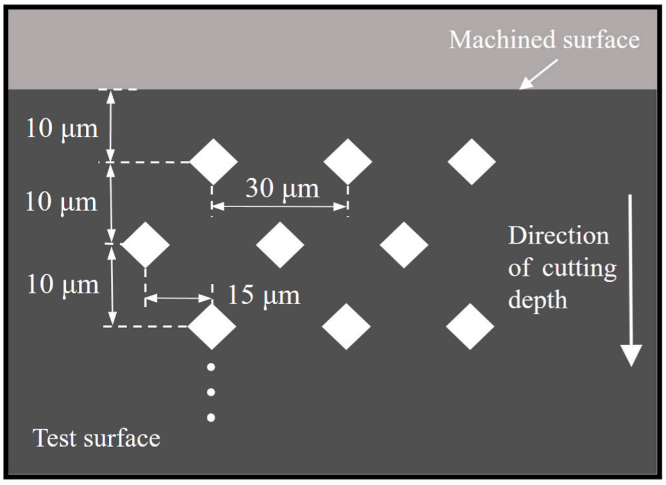

Fig. 5. Schematic diagram of the microhardness testing of machined surface layer.

surface, which is named as HR. And HR can be written as:

$$HR = \frac{MH - MH_0}{MH_0} \times 100\% \quad (3)$$

Where MH is the texted microhardness value of machined surface. MH_0 is the microhardness value of basis material, and the value is 323 HV.

3. Results and discussion

3.1. Microstructural plastic deformation of machined surface layer

In the cutting process, cutting force and cutting heat are the main factors to induce the plastic deformation of machined surface layer. Moreover, the depth of plastic deformation is positively correlated with the component of cutting force in cutting depth direction and the influence of cutting heat on the cutting depth direction. The microstructural plastic deformation of machined surface layer can be directly analysed by observing the metallographic diagram of machined surface layer. As can be seen from Fig. 6 (a), under the CC process, the plastic deformation depth of machined surface layer is 15.6 μm. Moreover, the grain has obvious distortion and elongation, and its deformation direction is consistent with the cutting direction. These results show that there is obvious plastic deformation in the titanium alloy machined surface layer during CC process. This is mainly because, in the CC process of titanium alloy, the cutting force of tool on workpiece is large. And, the heat dissipation effect is poor, the temperature apace rises in the cutting zone, so the thermal softening effect of machined surface layer material is remarkable. Therefore, the machined surface layer material deforms under the action of cutting force, and the deformation direction is consistent with the cutting direction. It is worth noting that the test result of machined surface layer plastic deformation is consistent with the analysis result of machined surface plastic side flow in our previous research [17], that is, in the CC process of titanium alloy, there are obvious plastic deformation of machined surface layer.

As shown in Fig. 6 (b), 6 (c) and 6 (d), under the UEVC processes, the plastic deformation depth values of machined surface layer are 8.6 μm, 6.3 μm and 5.9 μm, respectively, when the speed ratio is 1/12, 1/24 and 1/48. Compared with the CC process, the depth of plastic deformation of machined surface layer with UEVC process is significantly reduced, and decreases with the reduction of the speed ratio. This can be explained that the cutting force significantly decreases in the UEVC process due to intermittent cutting, the reduction of instantaneous cutting thickness and the increase of actual shear angle [13]. In addition, the cutting temperature of UEVC process is much lower than that of CC process because of the reduction of cutting force and the improvement of heat dissipation. In summary, in the UEVC process, the two main factors, cutting force and cutting heat that induce the plastic deformation of machined surface layer are significantly reduced. Moreover, in the UEVC process, the smaller speed ratio leads to the smaller cutting force and the better heat dissipation, which leads to the smaller plastic deformation depth of machined surface layer. It should be noted that, compared with the CC process, the grain distortion and elongation in the plastic deformation zone along the cutting direction is not obvious in the UEVC process, especially when the speed ratio is 1/48. This can be explained by the fact that, in the UEVC process, the cutting process is intermittent and the cutting direction is not consistent with the nominal cutting speed direction.

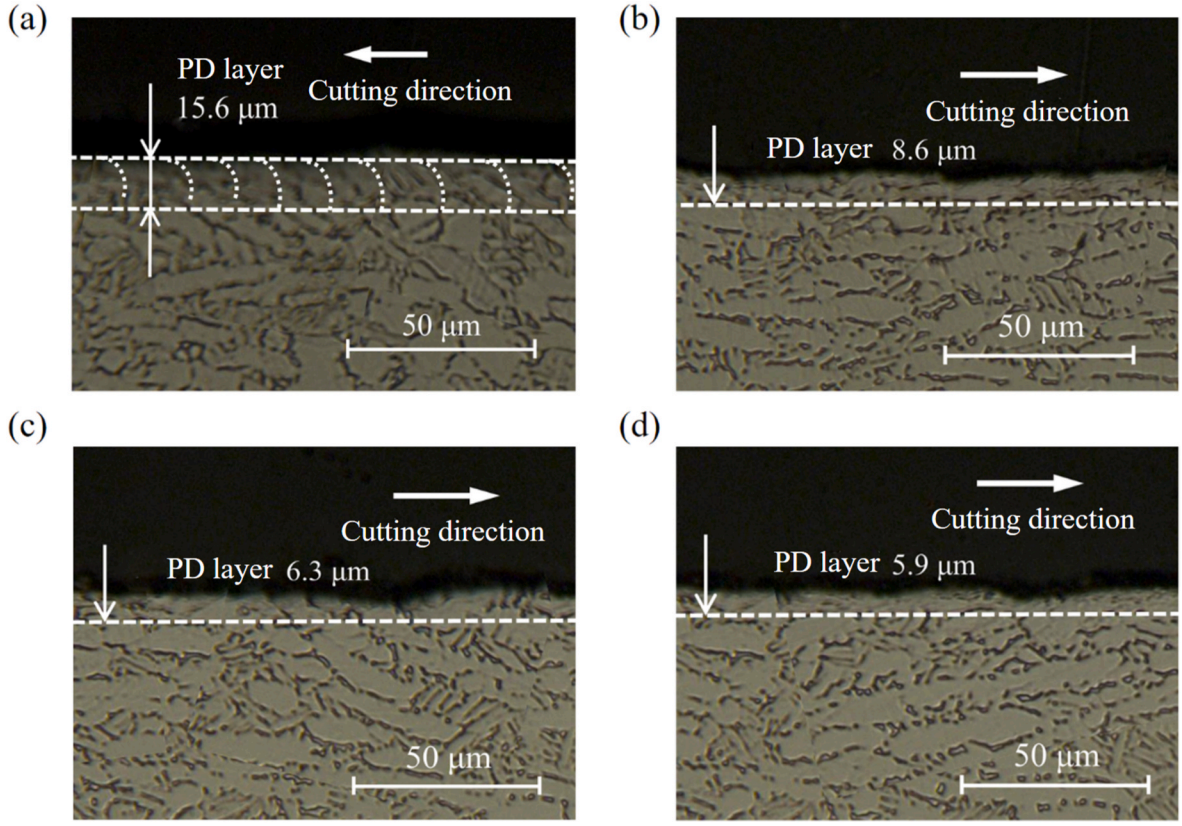

Fig. 6. Plastic deformation of the machined surface layer: (a) processed by CC, (b) processed by UEVC (R_S = 1/12), (c) processed by UEVC (R_S = 1/24) and (d) processed by UEVC (R_S = 1/48).

As can be seen from Fig. 6 (b), 6 (c) and 6 (d), in the plastic deformation zone, the grain arrangement is tight, the compression deformation is serious, and the grain boundary is blurred, and these phenomena are more obvious with the reduction of speed ratio. This can be interpreted as that, in the UEVC process, the cutting tool has an ultrasonic frequency impact on the workpiece in the cutting depth direction, the impact force on the machined surface is large because the action time is very short and the momentum of the ultrasonic oscillator is fixed. In addition, the contact area between cutting tool and workpiece is small, which makes the stress value acting on the machined surface larger. It is worth noting that under the action of high frequency and high stress, the machined surface layer material is easy to produce high strain rate, and high strain rate has obvious influence on the plastic deformation and the yield strength. A large number of dislocations are easily formed on the machined surface layer material due to the high frequency and high stress impact. It is obvious that the longitudinal development of plastic deformation can be limited by the increase of dislocation density. Thus, in the UEVC process, the plastic deformation depth is significantly reduced. In addition, in the UEVC process, the plastic deformation area show obvious compression deformation due to the impact of cutting tool on machined surface, that is, the grain arrangement is tight and the grain boundary is blurred. Moreover, the number of impact times per unit area is inversely proportional to the cutting speed. Therefore, with the reduction of speed ratio, the depth of plastic deformation layer is smaller and the compression deformation is more obvious.

3.2. Grain refinement of machined surface layer

As can be seen from Fig. 7, when the test line is 5 μm away from the machined surface, the grain size of the machined surface material under different processing methods are smaller than the initial grain size of the sample material (15.53 μm). According to the analysis results in section

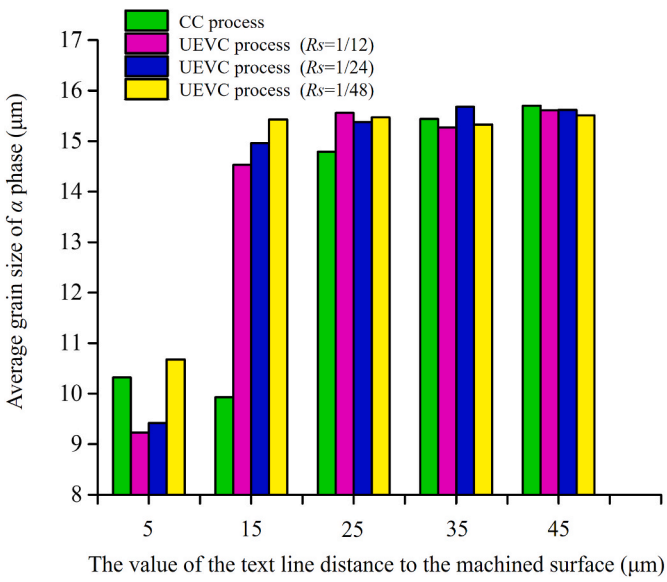

Fig. 7. Influence of the predetermined surface depth on the average grain size of α phase under different processing methods.

3.1, the grain is seriously deformed at the distance of 5 μm from machined surface, and the recrystallization may occurs under the action of strain energy, thus the grain size decreases. At the same time, the grain plastic deformation also makes the grain size decrease. It should be noted that compared with CC process, the grain size of surface layer machined by UEVC process is smaller. This is mainly because the cyclic impact of cutting tool causes serious compression plastic deformation of

the grain, so that the grain size becomes smaller. It can be predicted that the microhardness of plastic deformation material increases as the grain size decreases, and the study of microhardness will be carried out in section 3.4. The grain size of surface layer machined by CC process is still smaller than the initial grain size, when the test line is 15 μm away from the machined surface. However, the grain size of surface layer machined by UEVC process has little difference with the initial value. This result is consistent with the analysis in section 3.1, that is, the plastic deformation depth of machined surface layer is more than 15 μm under CC process, while the plastic deformation depth of machined surface layer is less than 10 μm under UEVC process. As can be seen from Fig. 7, when the test line is 25 μm away from the machined surface, there is a small difference in grain size between CC process and UEVC process. Moreover, the grain size tends to be the initial grain size as the test line is farther away from the machined surface. It is noteworthy that the grain size of surface layer machined by UEVC process has no obvious change with the reduction of the speed ratio. This can be interpreted as the cyclic impact of cutting tool is the main factor inducing grain deformation and size reduction. When the impact strength is certain, the small grain size promotes the hardness value increase of the surface material to increase, so as to reach the equilibrium state.

3.3. Phase transformation of machined surface layer

Ti–6Al–4V alloy has both α phase and β phase. The toughness of α phase is generally better than that of β phase, while the strength is lower than that of the β phase. During the cutting process, the machined surface layer material undergoes rapid changes in temperature and pressure, which induces the phase transformation. This causes the change of the ratio of α phase and β phase, which in turn causes the change of the physical and mechanical properties of the machined surface layer material. It is worth noting that α phase and β phase usually show different colour under the microscope. The quantitative analysis of the volume fraction of α phase and β phase can be completed through the digital processing of metallographic diagram. The details of the digital processing of metallographic diagram are recorded by the research results of Wang et al. [34], and the accuracy of this method has been confirmed. The metallographic structure diagram of the machined surface layer material and its corresponding figure obtained by the digital processing of metallographic diagram are shown in Fig. 8. As shown in Fig. 8(b), the volume proportion of α phase and β phase in the metallographic diagram can be obtained by counting the volume of white and black in the image. The phase transformation of the machined surface layer material can be obtained by calculating of the volume proportion of β phase per unit area along the cutting depth direction. The sampling area is set as a long strip (2μm × 200 μm). The metallographic information of the sample material used in this paper is tested, and the result shows that the volume fraction of β phase is 18.312%, which is consistent with the data given by the material supplier.

As can be seen from Fig. 9, under CC process, the volume fraction of β phase in the top layer of machined surface is as high as 39.758%, which is much higher than the content of β phase in basis material (18.312%). In addition, with the increase of machined surface layer depth value, the volume fraction of β phase decreases gradually. The phase transformation depth value of the machined surface layer material is about 8 μm, which is far less than the plastic deformation depth value. This can be explained by the fact that in CC process, the high temperature and high pressure in the cutting area promote the transformation of α phase into β phase, and the secondary α phase is precipitated from β phase during unloading and cooling. Significantly, the temperature of the area near the machined surface drops rapidly, and a small part of β phase precipitates into the secondary α phase. Therefore, in the area near machined surface, the volume fraction of α phase to β phase is greater than the volume fraction of β phase to secondary α phase, and this phenomenon is most obvious on the machined surface. This result is consistent with the analysis result in Section 3.1. There are a large number of long strip secondary α phase in the plastic deformation zone near the machined surface, as shown in Fig. 6 (a). The effect of cutting heat and cutting force on the phase transformation is weakened in the area farther from machined surface. It should be noted that with the increase of β phase volume fraction, its contribution to the macroscopic mechanical properties of the alloy also increases. In other words, under the CC process, the compression resistance of machined surface layer

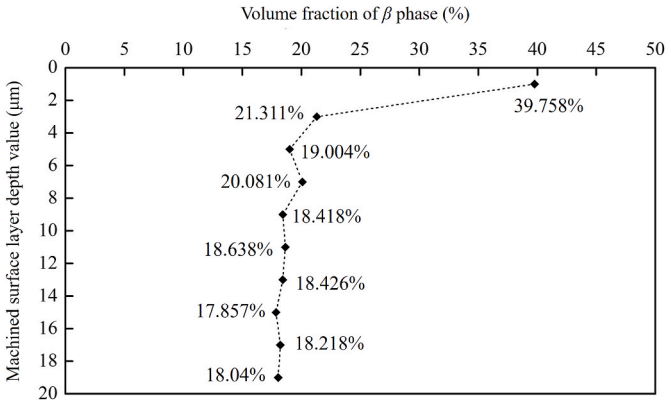

Fig. 9. Volume fraction of β phase with the machined surface layer depth value under CC process.

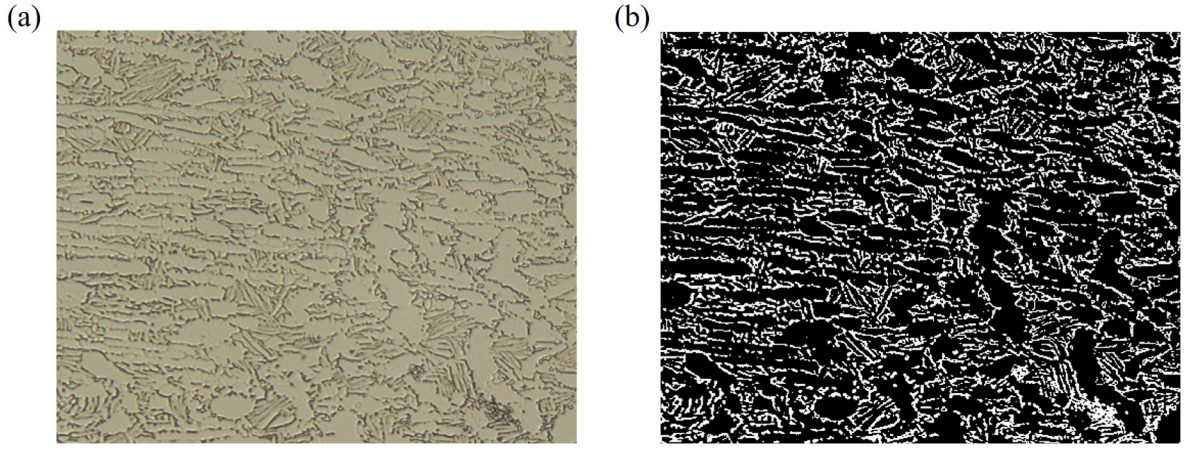

Fig. 8. Metallographic structure diagram of the machined surface layer material: (a) observed with the metallographic microscope, (b) obtained by the digital processing of metallographic diagram.

material is improved, and the plasticity is reduced. Correspondingly, the microhardness of the material in the area affected by the phase transformation is also changed, which will be analysed in Section 3.4.

As shown in Fig. 10, under the UEVC process, the volume fraction of β phase does not change significantly with the increase of the machined surface layer depth value, and it is basically equal to that of basis material. In addition, the speed ratio has little effect on the β phase volume fraction. This can be explained that, the cutting force and cutting heat, which induce the phase transformation of the machined surface layer material, are significantly reduced in the UEVC process. And the cutting force and cutting heat cannot meet the requirements of α phase transformation to β phase. In addition, it can be seen from Fig. 6 (b), 6 (c) and 6 (d) that there is no large number of long strip secondary α phase in the plastic deformation area. Therefore, in the UEVC process, the phase transformation of the machined surface layer material is obviously inhibited. It should be noted that the absence of phase transformation does not mean that the macroscopic mechanical properties do not change. The size and plastic deformation of the grains are also affect the mechanical properties of the machined surface layer material. In summary, the CC process, there is obvious phase transformation of the machined surface layer material. On the contrary, under the UEVC process, there is no obvious phase transformation on the machined surface layer material.

3.4. Microhardness of machined surface layer

In the CC process, the distribution curve of the microhardness of machined surface layer material is shown in Fig. 11 (a). In general, the microhardness value decreases with the increase of the depth value of machined surfaces layer, and returns to the same level as the basis material at the depth of 60 μm. These results show that the depth of the work hardening layer is 60 μm under the experimental parameters, and the work hardening effect in this area is stronger than the thermal softening effect. According to the analysis results in Section 3.1, 3.2 and 3.3, it can be seen that the increase of β phase volume fraction, grain plastic deformation and grain refinement are the main factors leading to hardening of the machined surface layer material. It should be noted that titanium compounds on the machined surface generated by chemical reactions between titanium alloy and air or cutting tool prompt the increase of microhardness. And, the microhardness of the machined surface is 364.8 HV. The microhardness value reaches the maximum (382.01 HV), when the distance from the machined surface is 10 μm. The above results show that there is an obvious thermal softening effect on titanium alloy machined surface under the CC process, and the influence depth of thermal softening effect is less than that of work hardening effect.

As shown in Fig. 11 (b), 11 (c) and 11 (d), in the UEVC process, when

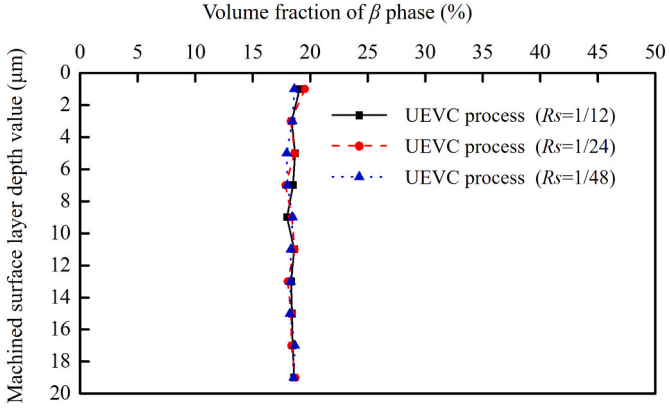

Fig. 10. Volume fraction of β phase with the machined surface layer depth value under UEVC processes with different cutting parameters.

R_S = 1/12, R_S = 1/24 and R_S = 1/48, the microhardness value of machined surface is 387.4 HV, 391.5 HV and 394.7 HV, respectively. Compared with CC process, the microhardness values of machined surfaces produced by UEVC technology increases significantly, and gradually increases with the decrease of speed ratio. This can be explained by the fact that, in the UEVC process, with the decrease of the speed ratio, the number of cutting tool impacts on machined surface per unit time increases, which results in tight grain arrangement and serious compression plastic deformation, as discussed in section 3.1. As we all know, the severely compressed plastic deformation region stores a lot of strain energy, which makes the deformation resistance of the plastic deformation material increase, that is, the microhardness value increases. Moreover, this phenomenon is most obvious in the machined surface. In addition, the microhardness value of the machined surface layer material decreases gradually with the distance from the machined surface, and which returns to the same level as the basis material at the depth of 50 μm. The result shows that the depth of work hardening layer is reduced by UEVC process compared with CC process. It should be noted that under the experimental parameters adopted in this study, the depth value of work hardening layer is not sensitive to the speed ratio. This can be interpreted as, in the UEVC process, the impact of cutting tool on the machined surface is the main factor leading to work hardening. And, the depth value of work hardening layer no longer changes significantly with the increase of impact number within a unit time, when the impact force reaches a certain value and the number of impacts exceeds the critical value. As shown in Fig. 11 (b), 11 (c) and 11 (d), in the UEVC process, the maximum microhardness appears on the machined surface. These results show that there is no obvious thermal softening effect on the machined surface layer material under the UEVC process. This is consistent with the previous analysis, that is, compared with the CC process, the cutting temperature is significantly reduced under the UEVC process.

Fig. 12 shows the hardening rate of the titanium alloy machined surface under different ultra-precision cutting methods. Under the experimental parameters adopted in this paper, the hardening rate of the titanium alloy machined surface with CC process is 13.32%. In the UEVC process, when R_S = 1/12, R_S = 1/24 and R_S = 1/48, the hardening rate of titanium alloy machined surface is 20.34%, 21.62% and 22.61%, respectively. The hardening rate of the titanium alloy machined surface with UEVC process is much greater than that of CC process. This can be explained by the fact that, in the UEVC process, the impact of cutting tool is the main factor leading to the increase of hardening rate. Moreover, in the CC process, the thermal softening effect is also one of the factors leading to the reduction of hardening rate. In addition, as shown in Fig. 12, in the UEVC process, the hardening rate of the titanium alloy machined surface increases with the decrease of speed ratio, and the increasing amplitude is small. This can be interpreted as, the increase of the impact number is the main factor leading to the increase of hardening rate, and when the impact number reaches a certain value, the increasing amplitude of hardening rate is small.

4. Conclusions

In this work, the evolution mechanism of microstructure and microhardness of Ti–6Al–4V alloy during CC and UEVC processes are studied and revealed. The significant conclusions of this work are concluded in following.

(1) Under the CC process, the grain has obvious distortion and elongation, and its deformation direction is consistent with the cutting direction. And the plastic deformation depth of machined surface layer is 15.6 μm. Compared with the CC process, the depth of plastic deformation of machined surface layer decreases with the reduction of the speed ratio, is less than 10 μm. Moreover, the plastic deformation area show obvious compression deformation due to the impact of cutting tool on machined

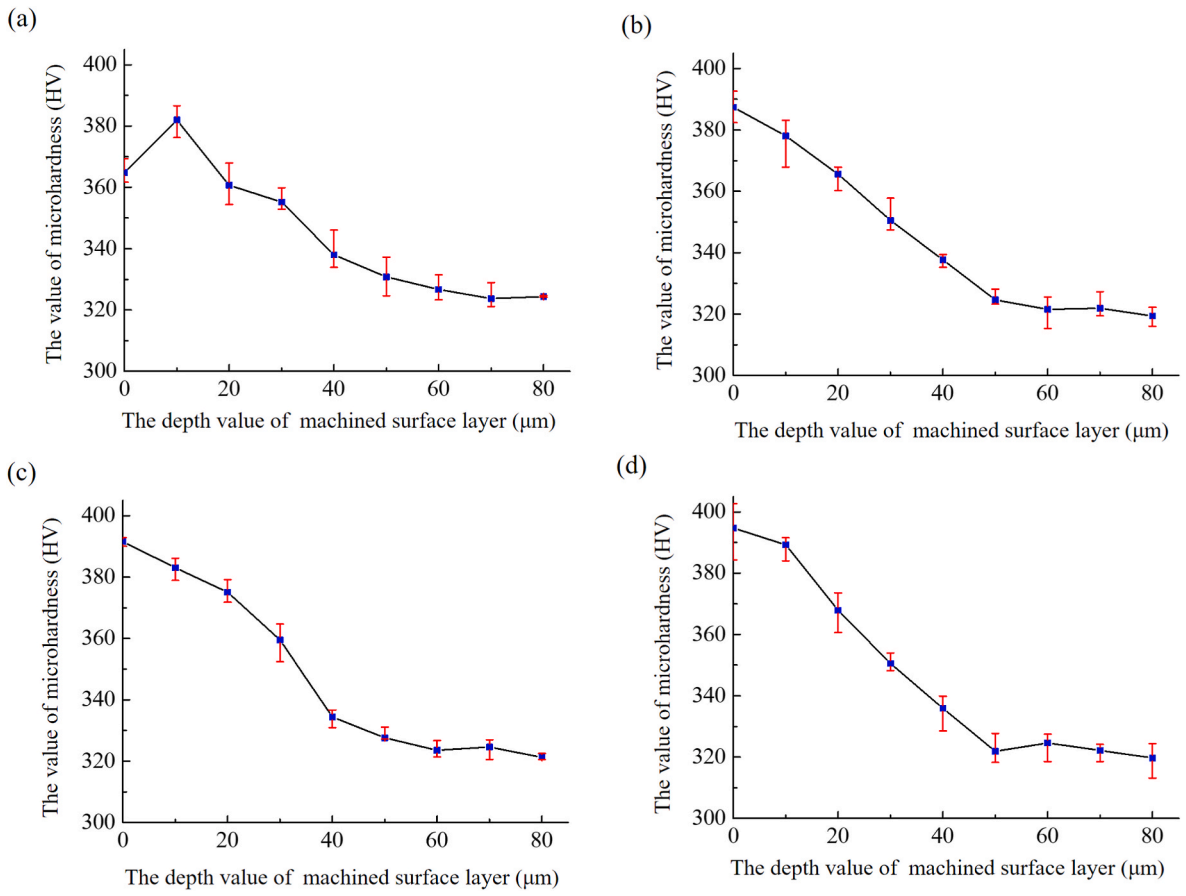

Fig. 11. Microhardness of the machined surface layer: (a) processed by CC, (b) processed by UEVC ($R_S = 1/12$), (c) processed by UEVC ($R_S = 1/24$) and (d) processed by UEVC ($R_S = 1/48$).

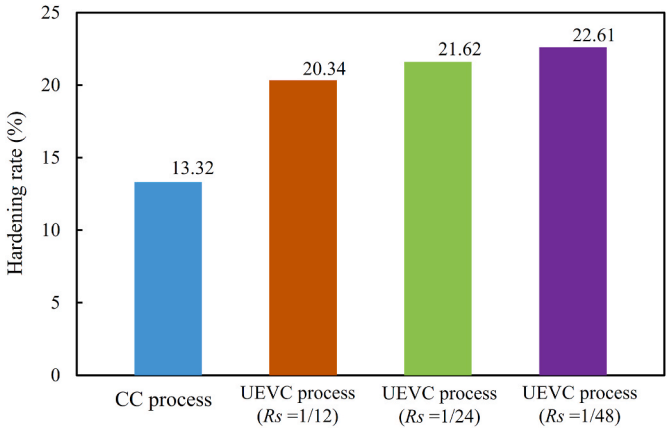

Fig. 12. The hardening rate of machined surface under different processing methods.

surface, that is, the grain arrangement is tight and the grain boundary is blurred, and these phenomena are more obvious with the reduction of speed ratio.

(2) Under CC and UEVC processes, the grain size of the machined surface material are smaller than the initial grain size of the sample material. And, compared with CC process, the grain size of surface layer machined by UEVC process is smaller. The grain size of surface layer machined by UEVC process has no obvious change with the reduction of the speed ratio. The cyclic impact of cutting tool is the main factor inducing grain deformation and size reduction. And, when the impact strength is certain, the small grain size promotes the hardness value increase of the surface material to increase, so as to reach the equilibrium state.

(3) To sum up, in the CC process, there is obvious phase transformation of the machined surface layer material. On the contrary, under the UEVC process, there is no obvious phase transformation on the machined surface layer material. The high temperature and high pressure in the cutting area are the main factors leading to the transformation of α phase into β phase.

(4) In the CC process, the work hardening effect is stronger than the thermal softening effect, there is an obvious thermal softening effect on machined surface, and the influence depth of thermal softening effect is less than that of work hardening effect. In the UEVC process, the impact of cutting tool on the machined surface is the main factor leading to work hardening. In the UEVC process, the hardening rate of the titanium alloy machined surface increases with the decrease of speed ratio, and it is more than 20%. In addition, compared with the CC process, there is no obvious thermal softening effect on the machined surface layer material under the UEVC process, and the depth of work hardening layer is signally reduced. For satisfying the high performance and high precision production of Ti–6Al–4V alloy part, the further investigations should be made for wear-resistant machined surface by optimizing the microscopic properties of machined surface layer material with the consideration of tool wear.

Declaration of competing interest

The authors declare that they have no known competing financial

interests or personal relationships that could have appeared to influence the work reported in this paper.

Acknowledgments

This paper was supported by Jiangxi Provincial Natural Science Foundation (Grant No. 20232BAB214056), Jiangxi Provincial Science and Technology Major Project (Grant No. 20223AAG02020), the National Natural Science Foundation of China (No. 52305497), Science and Technology Research Project of Jiangxi Provincial Department of Education (Grant No. GJJ210641), and Science Challenge Project of China (Grant No. TZ2018006-0202).

References

[1] Zhou X, Li Y, Han Z, Liu Z, Liu K, Tu Y, et al. Unusual stress-induced martensite transformation in Ti-6Al-4V alloy enabled by solution treatment in the lower α+ β regime. J Alloys Compd 2023;956:170330.
[2] Rossi MC, Kuroda PAB, de Almeida LS, Rossino LS, Afonso CRM. A detailed analysis of the structural, morphological characteristics and micro-abrasive wear behavior of nitrided layer produced in α (CP–Ti), α+ β (Ti–6Al–4V), and β (TNZ33) type Ti alloys. J. Mater. Res. Technol-JMRT 2023;27:2399–412.
[3] Ding Y, Kong L, Lei W, Li Q, Ding K, He Y. Study on the technology of surface strengthening Ti–6Al–4V alloy by near-dry multi-flow channel electrode electrical discharge machining. J. Mater. Res. Technol-JMRT 2024;28:2219–34.
[4] Elshaer RN, Ibrahim KM. Study of microstructure, mechanical properties, and corrosion behavior of as-cast Ni-Ti and Ti-6Al-4V alloys. J Mater Eng Perform 2023;32(17):7831–45.
[5] Khalil AK, Yip WS, To S. Theoretical and experimental investigations of magnetic field assisted ultra-precision machining of titanium alloys. J Mater Process Technol 2022;300:117429.
[6] Manjunath K, Tewary S, Khatri N, Cheng K. Simulation-based investigation on ultra-precision machining of additively manufactured Ti-6Al-4V ELI alloy and the associated experimental study. Proc Inst Mech Eng Part B-J Eng Manuf 2023. https://orcid.org/0000-0002-9558-8825.
[7] Tan R, Zhao X, Lin F, Jin S, Guo X, Chen X, Sun T. Analytical modelling and experimental study of surface roughness in ultrasonic elliptical vibration assisted ultra-precision cutting of Ti-6Al-4 V alloy. Int J Adv Manuf Technol 2023;126:1863–75.
[8] Yang K, Huang Q, Zhong B, Wang Q, Chen Q, Chen Y, et al. Enhanced extra-long life fatigue resistance of a bimodal titanium alloy by laser shock peening. Int J Fatig 2020;141:105868.
[9] De Angelis N, Solimei L, Pasquale C, Alvito L, Lagazzo A, Barberis F. Mechanical properties and corrosion resistance of TiAl6V4 alloy produced with SLM technique and used for customized mesh in bone augmentations. Appl. Sci.-Basel 2021;11(12):5622.
[10] Chen G, Ge J, Lu L, Liu J, Ren C. Mechanism of ultra-high-speed cutting of Ti-6Al-4V alloy considering time-dependent microstructure and mechanical behaviors. Int J Adv Manuf Technol 2021;113:193–213.
[11] Khalil AK, Yip WS, Rehan M, To S. A novel magnetic field assisted diamond turning of Ti-6Al-4 V alloy for sustainable ultra-precision machining. Mater Today Commun 2023;35:105829.
[12] Bai L, Yang Q, Cheng X, Ding Y, Xu J. A hybrid physics-data-driven surface roughness prediction model for ultra-precision machining. Sci China Technol Sci 2023;66(5):1289–303. https://doi.org/10.1007/s11431-022-2358-4.
[13] Zhang XQ, Liu K, Kumar AS, Rahman M. A study of the diamond tool wear suppression mechanism in vibration-assisted machining of steel. J Mater Process Technol 2014;214:496–506.
[14] Peng Z, Zhang X, Zhang D. Performance evaluation of high-speed ultrasonic vibration cutting for improving machinability of Inconel 718 with coated carbide tools. Tribol Int 2021;155:106766.
[15] Bai J, Xu Z, Qian L. Precision-improving manufacturing produces ordered ultra-fine grained surface layer of tungsten heavy alloy through ultrasonic elliptical vibration cutting. Mater Des 2022;220:110859.
[16] Tan RK, Zhao XS, Zhang S, Zou XC, Guo SS, Hu ZJ, Sun T. Study on ultra-precision processing of Ti-6Al-4V with different ultrasonic vibration-assisted cutting modes. Mater Manuf Process 2019;34(12):1380–8.
[17] Tan RK, Zhao XS, Sun T, Zou XC, Hu ZJ. Experimental investigation on micro-groove manufacturing of Ti-6Al-4V alloy by using ultrasonic elliptical vibration assisted cutting. Materials 2019;12:3086.
[18] Tan R, Zhao X, Guo S, Zou X, He Y, Geng Y, et al. Sustainable production of dry-ultra-precision machining of Ti–6Al–4V alloy using PCD tool under ultrasonic elliptical vibration-assisted cutting. J Clean Prod 2020;248:119254.
[19] Wang H, Kang R, Bao Y, Wang K, Guo X, Dong Z. Microstructure evolution mechanism of tungsten induced by ultrasonic elliptical vibration cutting at atomic/nano scale. Int J Mech Sci 2023;253:108397.
[20] Jin X, Lan L, Gao S, He B, Rong Y. Effects of laser shock peening on microstructure and fatigue behavior of Ti–6Al–4V alloy fabricated via electron beam melting. Mater. Sci. Eng. A-Struct. Mater. Prop. Microstruct. Process. 2020;780:139199.
[21] Wu Z, Kou H, Tang L, Chen W, Han X, Deng Y, et al. Microstructural effects on the high-cycle fatigue and fracture behaviors of Ti-6Al-4V alloy. Eng Fract Mech 2020;235:107129.
[22] Wen Y, Bi J, Zhou J, Guo H, Yi J, Wang L, Hua L, Xie L. Influence mechanism of microstructure variation on mechanical properties of laser melting deposition Ti-6Al-4V alloy under electroshocking treatment. J. Mater. Res. Technol-JMRT. 2023;25:2758–68.
[23] Hou N, Wang M, Zhang Y, Wang H, Song C. Insights into the fatigue property of titanium alloy Ti-6Al-4V in aero-engine from the subsurface damages induced by milling: state of the art. Int J Adv Manuf Technol 2021;113:1229–35.
[24] Wang ZY, Ren JX, Zhou JH, Cai J. Correlation analysis of microstructure evolution on microhardness and residual stress for cutting Ti-6Al-4V titanium alloy. Proc Inst Mech Eng Part B-J Eng Manuf 2023;237(6–7):885–98.
[25] Safari H, Sharif S, Izman S, Jafari H. Surface integrity characterization in high-speed dry end milling of Ti-6Al-4V titanium alloy. Int J Adv Manuf Technol 2015;78:651–7.
[26] Patil S, Jadhav S, Kekade S, Supare A, Powar A, Singh RKP. The influence of cutting heat on the surface integrity during machining of titanium alloy ti6al4v. Procedia Manuf 2016;5:857–69.
[27] Rotella G, Dillon OW, Umbrello D, Settineri L, Jawahir IS. The effects of cooling conditions on surface integrity in machining of Ti6Al4V alloy. Int J Adv Manuf Technol 2014;71:47–55.
[28] Wang Q, Liu Z, Wang B, Song Q, Wan Y. Evolutions of grain size and micro-hardness during chip formation and machined surface generation for Ti-6Al-4V in high-speed machining. Int J Adv Manuf Technol 2016;82:1725–36.
[29] Moussaoui K, Mousseigne M, Senatore J, Chieragatti R, Monies F. Influence of milling on surface integrity of Ti6Al4V-study of the metallurgical characteristics: microstructure and microhardness. Int J Adv Manuf Technol 2013;67:1477–89.
[30] Bai W, Sun R, Leopold J, Silberschmidt VV. Microstructural evolution of Ti6Al4V in ultrasonically assisted cutting: numerical modelling and experimental analysis. Ultrasonics 2017;78:70–82.
[31] Sun Z, Geng D, Guo H, Zhang Q, Liu Y, Liu L, Jiiang X, Zhang D. Introducing transversal vibration in twist drilling: material removal mechanisms and surface integrity. J Mater Process Technol 2024;325:118296.
[32] Geng D, Sun Z, Liu Y, Liu L, Cai J, Jiang X, Zhang D. Unravelling the influence of vibration on material removal and microstructure evolution in ultrasonic transversal vibration-assisted helical milling of Ti-6Al-4V holes. J Mater Process Technol 2024;326:118320.
[33] Ying E, Zhou Z, Geng D, Shao Z, Sun Z, Liu Y, Liu L, Jiiang X, Zhang D. High-efficiency ultrasonic assisted drilling of CFRP/Ti stacks under non-separation type and dry conditions. J Zhejiang Univ - Sci 2024:1–17. https://jzus.zju.edu.cn/iparticle.php?doi=10.1631/jzus.A2300227.
[34] Zhang XP, Shivpuri R, Srivastava AK. Role of phase transformation in chip segmentation during high speed machining of dual phase titanium alloys. J Mater Process Technol 2014;214:3048–66.
[35] Pan Z, Liang SY, Garmestani H, Shih DS. Prediction of machining-induced phase transformation and grain growth of Ti-6Al-4V alloy. Int J Adv Manuf Technol 2016;87:859–66.
[36] Wang Q, Liu Z. Stress-induced orientation relationship variation for phase transformation of α-Ti to β-Ti during high speed machining Ti-6Al-4V. Mater. Sci. Eng. A-Struct. Mater. Prop. Microstruct. Process. 2017;690:32–6.
[37] Wang Q, Liu Z, Yang D, Mohsan AUH. Metallurgical-based prediction of stress-temperature induced rapid heating and cooling phase transformations for high speed machining Ti-6Al-4V alloy. Mater Des 2017;119:208–18.
[38] Nath C, Rahman M, Neo KS. Machinability study of tungsten carbide using PCD tools under ultrasonic elliptical vibration cutting. Int J Mach Tool Manufact 2009;49:1089–95.
[39] Yip WS, To S. Ductile and brittle transition behavior of titanium alloys in ultra-precision machining. Sci Rep 2018;8:3934.
[40] Tan R, Zhao X, Zou X, Sun T. A novel ultrasonic elliptical vibration cutting device based on a sandwiched and symmetrical structure. Int J Adv Manuf Technol 2018;97:1397–406.